Rosuvastatin Liver Partitioning in Cynomolgus Monkeys: Measurement In Vivo and Prediction Using In Vitro Monkey Hepatocyte Uptake

Bridget L. Morse, Hong Cai,[1] Jamus G. MacGuire, Maxine Fox, Lisa Zhang, Yueping Zhang, Xiaomei Gu, Hong Shen, Elizabeth A. Dierks, Hong Su, Chiuwa E. Luk, Punit Marathe, Yue-Zhong Shu, W. Griffith Humphreys, and Yurong Lai

Pharmaceutical Candidate Optimization (B.L.M., H.C., L.Z., Y.Z., X.G., H.S., E.A.D., H.S., C.E.L., P.M., Y-Z.S., W.G.H., Y.L.) and Veterinary Sciences, Bristol-Myers Squibb, Princeton, New Jersey (J.G.M., M.F.)

ABSTRACT

Unbound plasma concentrations may not reflect those in target tissues, and there is a need for methods to predict tissue partitioning. Here, we investigate the unbound liver partitioning ($Kp_{u,u}$) of rosuvastatin, a substrate of hepatic organic anion transporting peptides, in cynomolgus monkeys and compare it with that determined using hepatocytes in vitro. Rosuvastatin (3 mg/kg) was administered orally to monkeys and plasma and liver (by ultrasound-guided biopsy) collected over time. Uptake into monkey hepatocytes was evaluated up to steady state. Binding in monkey plasma, liver, and hepatocytes was determined using equilibrium dialysis. Mean in vivo $Kp_{u,u}$ was 118 after correcting total liver partitioning by plasma and liver binding. In vitro uptake data were analyzed by compartmental modeling to determine active uptake clearance, passive diffusion, the intracellular unbound fraction, and $Kp_{u,u}$. In vitro $Kp_{u,u}$ underpredicted that in vivo, resulting in the need for an empirical in vitro to in vivo scaling factor of 10. Adjusting model parameters using hypothetical scaling factors for transporter expression and surface area or assuming no effect of protein binding on active transport increased partitioning values by 1.1-, 6-, and 9-fold, respectively. In conclusion, in vivo rosuvastatin unbound liver partitioning in monkeys was underpredicted using hepatocytes in vitro. Modeling approaches that allow integrating corrections from passive diffusion or protein binding on active uptake could improve the estimation of in vivo intracellular partitioning of this organic anion transporting peptide substrate. A similar assessment of other active hepatic transport mechanisms could confirm and determine the extent to which limited accumulation in isolated hepatocytes needs to be considered in drug development.

Introduction

Recent progress toward understanding drug transport has called into question previous assumptions of drug disposition and tissue accumulation. Specifically, the underlying principles of active transport allow unbound concentrations across a membrane to differ, undermining the notion that unbound plasma concentrations equal those in tissue and may therefore serve as a surrogate for unbound tissue concentrations. As tissue concentrations are directly responsible for many effects pertaining to drug safety and efficacy, of late, there has been increasing emphasis placed on methods for measuring or predicting tissue drug concentrations, particularly for compounds whose disposition is governed by drug transporters (Chu et al., 2013b).

Although noninvasive imaging for monitoring target tissue concentrations is now feasible for some therapeutic agents in the clinic (Bauer et al., 2012; van Velden et al., 2015), methods to predict intracellular tissue concentrations are needed in drug discovery and development. Although total tissue partitioning can be readily measured in rodents, there are noted interspecies differences in hepatic transporter homology and expression between rodents and humans (Chu et al., 2013a); therefore, it cannot be assumed that tissue partitioning in humans can be reliably predicted directly from that in rodents. Additionally, methods for measuring tissue concentrations in vivo do not enable measurement of *unbound* concentrations, which are responsible for drug effects. As such, in vitro methods for predicting intracellular unbound concentrations and unbound tissue partitioning are sought after.

As the liver is often the site of drug action and toxicity, attention has focused on the use of hepatocytes in vitro for predicting unbound liver partitioning in vivo. A number of approaches have been described using rat or human hepatocytes for the uptake of substrates for the hepatic

---

ABBREVIATIONS: KHB, Krebs-Henseleit buffer; *Kp*, total tissue partition coefficient; $Kp_{u,u}$, unbound tissue partition coefficient; LC-MS/MS, liquid chromotography–mass spectrometry; OATP, organic anion transporting polypeptide.

organic anion transporting polypeptides (OATPs) (Paine et al., 2008; Yabe et al., 2011; Nordell et al., 2013; Pfeifer et al., 2013; Shitara et al., 2013; Keemink et al., 2015). Approaches that have compared in vitro partitioning in rat hepatocytes to that in the rat liver in situ or in vivo conclude a generally good prediction for select compounds (Paine et al., 2008; Pfeifer et al., 2013). However, as mentioned, rat orthologs of the OATP family differ considerably in amino acid sequence and tissue distribution compared with the human isoforms (Hagenbuch and Meier, 2004) and uptake into human hepatocytes has been demonstrated considerably lower than that in the rat for a number of OATP substrates (Poirier et al., 2009; Menochet et al., 2012b). Additionally, in vitro to in vivo extrapolation in rats is generally assessed using fresh hepatocytes, for which human materials are at best impractical in drug discovery and development. These discrepancies beg the question of the suitability of methods validated for the prediction of partitioning in the rat for the prediction of liver partitioning using human cryopreserved hepatocytes. Recently, Shen et al. cloned and characterized OATP1B1, OATP1B3, and OATP2B1 in cynomolgus monkeys, demonstrating these isoforms share >90% amino acid identity with human OATPs, along with a similar uptake/inhibition activity for probe compounds (Shen et al., 2013). Furthermore, for rosuvastatin, a broad substrate of monkey and human OATPs, similar transport kinetics were observed in monkey and human cryopreserved hepatocytes and a similar in vivo disposition and OATP-mediated interactions for rosuvastatin in humans were quantitatively reproduced using monkeys (Shen et al., 2013, 2015). In this research, we demonstrate the use of a novel method for liver sampling in cynomolgus monkeys and evaluate the monkey as a model for in vitro to in vivo extrapolation of rosuvastatin unbound liver partitioning.

Materials and Methods

Chemicals

Rosuvastatin was purchased from Toronto Research Chemicals (North York, ON, Canada). Carbamazepine and rifamycin SV were purchased from Sigma-Aldrich (St. Louis, MO). InVitroGRO HT medium and Krebs-Henseleit buffer (KHB) were purchased from Bioreclamation IVT (Baltimore, MD). All other chemicals and reagents were of analytical grade.

In Vivo Rosuvastatin Pharmacokinetic Study in Monkeys. Animal studies were approved by the Bristol-Myers Squibb Institutional Animal Care and Use Committee and performed under the standards recommended by the *Guide for the Care and Use of Laboratory Animals*. Male cynomolgus monkeys were obtained from BioCulture (Mauritius) Ltd. (Riviere de Anguilles, Mauritius). Monkeys ($n = 3$; 6–8 kg) were fasted overnight starting at 3 p.m. Then, the following morning, they were dosed with rosuvastatin (3 mg/kg) in solution by oral gavage. Blood and liver samples were taken at 1, 6, and 24 hours after rosuvastatin administration. Blood samples (3–5 ml/time point) were collected from a central venous port into EDTA tubes and immediately spun to collect plasma. Liver samples were collected by ultrasound-guided biopsy. Monkeys were administered ketamine (5–10 mg/kg) and dexmedetomidine (0.02 mg/kg) intramuscularly prior to the biopsy procedure. Throughout the procedure, the anesthetic depth was monitored by toe pinch reflex, gross purposeful movement, and palpebral reflex. For local analgesia, 0.1–0.2 ml of 2% lidocaine was subcutaneously injected at the biopsy site. With the monkey in a dorsal recumbent position, hair was clipped from the right cranial abdomen and skin disinfection was conducted. A routine transabdominal ultrasound was conducted to identify an appropriate liver biopsy site free of great vessels, the gallbladder, and adjacent organs. Samples were taken from the right medial or right lateral lobe. A sterile 18-gauge biopsy needle was slowly advanced under the skin until it was visualized at the appropriate biopsy site and then the spring-loaded biopsy apparatus was discharged to obtain a core of the liver tissue (~4–8 mg). At completion of the procedure, ultrasound visualization of the biopsy site was maintained to check for signs of hemorrhaging and dexmedetomidine was reversed using atipamezole (0.15 mg/kg). One liver sample was taken from one monkey at each time point ($n = 1$/time point). Three weeks later, the procedure was repeated in the same animals. Blood samples were again collected 1, 6, and 24 hours postdose in all animals and one liver sample was again

collected from one animal at 1, 6, and 24 hours ($n = 1$/time point). The liver sampling was staggered so that the same time point was not collected from the same animal on the two study days. On each study day, the animals were fed at approximately 8 hours postdose. Liver samples were snap frozen on dry ice, and all samples were stored at −80°C until rosuvastatin concentrations were determined by liquid chromotography–mass spectrometry (LC-MS/MS).

In Vitro Uptake of Rosuvastatin in Monkey Hepatocytes

Uptake of rosuvastatin was evaluated in monkey hepatocytes in suspension using the oil-spin method. Female cynomolgus monkey cryopreserved hepatocytes (10 female-pooled lot #012-1407) were purchased from In Vitro ADMET Laboratories, LLC (Columbia, MD). Hepatocytes were thawed at 37°C and then placed in InVitroGRO HT medium. Cells were spun down and reconstituted in KHB to a density of 2×10^6 viable cells/ml. Cell viability was >90%, as determined by Trypan blue staining. Rosuvastatin uptake was evaluated from 0.25 to 15 minutes at 0.2 and 1 μM at 37°C and at 1 μM at 4°C. As uptake at 4°C may underestimate passive diffusion (Poirier et al., 2008), uptake was also assessed at 37°C in the absence and presence of 100 μM rifamycin SV from 0.25 to 1.5 minutes. All time points were evaluated in triplicate. For evaluation at 37°C, cells were prewarmed for 3 minutes prior to the initiation of rosuvastatin uptake. For evaluation at 4°C, cells were kept on ice after reconstitution. To initiate uptake, an equal volume of KHB containing 2× the rosuvastatin concentration was added. Aliquots were taken at specified time points and added to centrifuge tubes containing 100 μl of a 5:1 silicone to mineral oil ratio (density = 1.015) and 50 μl of 2 M ammonium acetate and then spun down using table-top centrifuges at 10,000 rpm for 10 seconds to stop transport. Tubes were immediately placed on dry ice and stored at −80°C until rosuvastatin concentrations were determined by LC-MS/MS.

In Vitro Binding

Binding of rosuvastatin in monkey plasma, liver, and hepatocyte lysate was determined using equilibrium dialysis. All samples were isolated from in-house animals. The hepatocytes used were cryopreserved cells that were isolated from liver samples using the two-step collagenase perfusion method (Berry and Friend, 1969). All matrices were evaluated at 1 μM rosuvastatin in quadruplicate. Binding in plasma was evaluated with no dilution. Liver binding was evaluated in 2-, 4-, and 8-fold diluted homogenate. Cryopreserved hepatocytes were thawed at 37°C in InVitroGRO HT and reconstituted to 15×10^6 cells/ml in KHB. The cells were killed by several freeze/thaw cycles, followed by hydrolytic lysis. They were then reconstituted and diluted to 1, 5, and 15×10^6 cells/ml for binding experiments. All dilutions were made in 133 mM sodium phosphate buffer. Equilibrium dialysis was carried out in a 96-well microequilibrium dialysis device (HTDialysis, LLC, Gales Ferry, CT). Prior to equilibration, membranes of 12–14 kDa cutoff were placed in distilled water for 30 minutes, followed by sodium phosphate buffer for 30 minutes. After aligning the membranes in the apparatus, 150 μl of each matrix sample was pipetted opposite 150 μl of sodium phosphate buffer and incubated at 37°C for 4 hours. As rosuvastatin may undergo metabolism/interconversion to rosuvastatin lactone, the stability of rosuvastatin acid over 4 hours was evaluated by incubating rosuvastatin in separate samples in all matrices at each dilution and similarly incubating at 37°C. Recovery of rosuvastatin acid from these samples was 89–103% in the various matrices, indicating little interconversion in vitro. After 4 hours, 20 μl of the matrix sample and 50 μl of buffer were taken. The matrix sample was added to 50 μl of blank buffer, and buffer was added to 20 μl of blank matrix to maintain a similar composition between the buffer and samples for the determination of rosuvastatin concentrations by LC-MS/MS. From diluted matrices, undiluted fraction unbound was determined as previously described (Kalvass and Maurer, 2002). For hepatocytes, the dilution factor was determined by using a value of 1 mg protein/10^6 cells, which was compared with the protein concentration measured in whole monkey liver via spectrophotometric assay. All samples were stored at −80°C until rosuvastatin concentrations were determined by LC-MS/MS.

LC-MS/MS Measurement of Rosuvastatin

In Vivo Samples. Liver samples were homogenized 1:5 in distilled water. One hundred microliters of the homogenized sample was mixed with 200 μl of

acetonitrile containing the internal standard (100 nM rosuvastatin-d6). Samples were then vortexed and centrifuged for 10 minutes at 3500 rpm. The supernatant was then dried under nitrogen gas and reconstituted in 50 μl of mobile phase A. Plasma and liver standard curves were prepared by adding 10 μl of 10× standard into 90 μl of blank plasma or liver homogenate, and then precipitated, dried, and reconstituted similarly to the samples. In vivo samples were run on a high-performance liquid chromatography system consisting of a Shimadzu LC-10AD VP pump (Shimadzu Corp., Kyoto, Japan) and HTC Pal autosampler (CTC Analytics AG, Zwingen, Switzerland). The HPLC system was connected to an AB Sciex 4000 QTrap mass spectrometer (MDS Sciex, Concord, ON, Canada). Five microliters of the sample were injected onto an Atlantis dC18 column (5 μm, 2.1 × 10 mm) (Waters Corp., Millford, MA). Mobile phases were 0.1% formic acid in water and 0.1% formic acid in acetonitrile. Elution of rosuvastatin and rosuvastatin-d6 was achieved with the following gradient at a flow rate of 0.4 ml/min: 10% B to 60% B over 3 minutes, 60% B maintained from 3 to 3.5 minutes, 60% B to 90% B from 3.5 to 3.6 minutes, 90% B maintained from 3.6 to 4 minutes, return to 10% B from 4 to 4.1 minutes, and 10% B maintained from 4.1 to 4.5 minutes. Multiple reaction monitoring mass transitions were 482.2→270.2 and 488.2→276.2 for rosuvastatin and rosuvastatin-d6, respectively, in the positive mode. The calibration curves for plasma and liver ranged from 2 to 1000 nM (r^2 = 0.999 and 0.997 for plasma and liver, respectively).

In Vitro Samples. Hepatocyte pellets were cut from microcentrifuge tubes and sonicated following the addition of 100 μl of distilled water for 15 minutes. The internal standard (100 nM carbamazepine) in 200 μl of acetonitrile was then added, and samples were vortexed for 30 minutes. Standards were prepared by adding stock solution to blank hepatocyte pellets, and then were treated similarly to hepatocyte samples. A 225-μl aliquot of the standard and samples was filtered through a 0.45-μm hydrophilic low-binding polytetrafluoroethylene filter plate, and then the filtrates were dried under nitrogen gas and reconstituted in 150 μl of a 4:1 mobile phase A to B ratio. Plasma, liver, and hepatocyte lysate samples from in vitro binding experiments were quantitated with a standard curve made in a similar matrix (5:2, blank buffer to matrix ratio). To the 70 μl of each sample or standard, 200 μl of acetonitrile-containing internal standard (100 nM carbamazepine) was added and samples were vortexed. A 200-μl aliquot of each was then filtered through a 0.45-μm hydrophilic low-binding PTFE filter plate, and then the filtrates were dried under nitrogen gas and reconstituted in 150 μl of the 4:1 mobile phase A to B ratio. In vitro samples were run on a Shimadzu UPLC system (Shimadzu Corp.) connected to an AB Sciex 6500 Qtrap mass spectrometer (MDS Sciex). Five microliters of the sample were injected onto an Atlantis dC18 column (5 μm, 2.1 × 10 mm). Mobile phases were 0.1% formic acid in water (A) and acetonitrile (B). Elution of rosuvastatin and the internal standard was achieved with the following gradient: 15% B to 60% B over 2 minutes, 60% B to 95% B from 2 to 2.5 minutes, 95% B maintained from 2.5 to 3 minutes, return to 15% B from 3 to 3.1 minutes, and 15% B maintained from 3.1 to 5 minutes. Multiple reaction monitoring mass transitions were 482.2→258.2 and 237.1→194.0 for rosuvastatin and carbamazepine, respectively, in the positive mode. The calibration curves for all matrices ranged from 1 to 1000 nM (r^2 = 0.993–1.0).

Data Analysis

Total in vivo liver partitioning (Kp) for rosuvastatin was determined for each liver and corresponding plasma sample and over time with eqs. 1 and 2, respectively

$$Kp = \frac{C_{liver}}{C_{plasma}} \tag{1}$$

$$Kp = \frac{AUC_{liver}}{AUC_{plasma}} \tag{2}$$

where C_{liver} and C_{plasma} represent the total rosuvastatin concentration in the liver and plasma. The area under the concentration time curve values of rosuvastatin were calculated from 0 to 24 hours using the Bailer method in Phoenix WinNonLin 6.3 (Certara L.P., Princeton, NJ). Unbound liver partitioning ($Kp_{u,u}$) was determined with eq. 3

$$Kp_{u,u} = Kp \cdot \frac{fu_{liver}}{fu_{plasma}} \tag{3}$$

where fu_{liver} and fu_{plasma} represent the unbound fraction in monkey liver and plasma, respectively, as determined by equilibrium dialysis.

Mathematical modeling of the in vitro rosuvastatin uptake was performed using a two-compartment model, similar to those previously described (Poirier et al., 2008; Menochet et al., 2012a). The total intracellular amount in each hepatocyte sample was determined by multiplying the measured rosuvastatin concentration by the reconstitution volume. Total intracellular concentrations were then calculated from total intracellular amounts, assuming a cell volume of 4 μl/10^6 cells (Reinoso et al., 2001). As changes in rosuvastatin medium concentrations over time were not expected in these experiments, the medium concentration was not measured and only the intracellular rosuvastatin concentrations were included in the model fitting. All modeling was performed using Phoenix WinNonLin 6.3 (Certara L.P.). The model structure is shown in Fig. 1. Model equations are as below for uptake at 37°C:

$$dC_{medium}/dt = \frac{-C_{medium} \cdot fu_{medium} \cdot (Cl_{up} + PS_{diff}) + C_{cell} \cdot fu_{cell} \cdot PS_{diff}}{V_{medium}} \tag{4}$$

$$dC_{cell}/dt = \frac{C_{medium} \cdot fu_{medium} \cdot (Cl_{up} + PS_{diff}) - C_{cell} \cdot fu_{cell} \cdot PS_{diff}}{V_{cell}} \tag{5}$$

and at 4 and 37°C with rifamycin SV

$$dC_{medium}/dt = \frac{-C_{medium} \cdot fu_{medium} \cdot PS_{diff} + C_{cell} \cdot fu_{cell} \cdot PS_{diff}}{V_{medium}} \tag{6}$$

$$dC_{cell}/dt = \frac{C_{medium} \cdot fu_{medium} \cdot PS_{diff} - C_{cell} \cdot fu_{cell} \cdot PS_{diff}}{V_{cell}} \tag{7}$$

where C_{medium} and C_{cell} represent the total rosuvastatin concentration in the medium and intracellular compartments, respectively; V_{medium} and V_{cell} represent the volume of the medium and intracellular compartments, respectively; fu_{medium} and fu_{cell} represent the unbound fraction in the medium and intracellular compartments, respectively; Cl_{up} represents the unbound active uptake clearance; and PS_{diff} represents the unbound passive diffusion clearance. V_{cell} and V_{medium} were fixed to 4 and 1000 μl/10^6 cells, respectively. Rosuvastatin was presumed to be completely unbound in the medium, and fu_{medium} was fixed to 1. Fitted parameters included PS_{diff}, Cl_{up}, and fu_{cell}. We further evaluated the effect of varying fu_{cell} values on the fitted clearance parameters by fixing fu_{cell} from 0.05 to 1 and fitting Cl_{up} and PS_{diff}, which could be estimated using only data at 37°C when fu_{cell} was fixed. Initial conditions for the intracellular compartment were fixed at the intercept at time = 0, which was determined by linear regression using the initial linear uptake rate, and initial conditions for the medium compartment were fixed to the nominal rosuvastatin concentration added prior to initiation of uptake. Rosuvastatin medium concentrations over time were simulated using the obtained fitted parameters to validate the assumption of negligible change in this compartment. Any simulated changes in C_{medium} were included in the calculation of in vitro Kp and $Kp_{u,u}$, which were determined as below, using C_{cell} and C_{medium} at 15 minutes after steady state was obtained
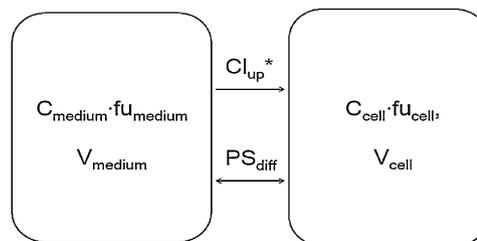
Fig. 1. In vitro model structure. Model parameters (Cl_{up}, PS_{diff}, and fu_{cell}) were fit to measured intracellular rosuvastatin concentrations using hepatocyte uptake data at 37 and 4°C, simultaneously. *Cl_{up} included only for data at 37°C, as indicated in model equations under *Materials and Methods*. C_{medium}, fu_{medium}, and V_{medium} represent the rosuvastatin concentration, fraction unbound, and volume in the medium compartment, respectively. C_{cell}, fu_{cell}, and V_{cell} represent the rosuvastatin concentration, fraction unbound, and volume in the intracellular compartment, respectively. Cl_{up} and PS_{diff} represent unbound active and unbound diffusion clearance, respectively.

$$Kp = \frac{C_{\text{cell}}}{C_{\text{medium}}} \quad (8)$$

$$Kp_{u,u} = Kp \cdot fu_{\text{cell}} \quad (9)$$

Following the estimation of in vitro parameters, simulations using the two-compartment model were performed to test various hypotheses to explain observed in vitro to in vivo discrepancy in $Kp_{u,u}$. In these simulations, the volumes of the extracellular and intracellular compartments were fixed to those for plasma and liver, respectively, of a 5-kg monkey (Bischoff et al., 1971). The in vitro clearance parameters determined using the two-compartment model were scaled up to that of the whole liver by similarly using the physiologic values for a 5-kg cynomolgus monkey and published scaling factor for hepatocellularity (Bischoff et al., 1971; Houston, 1994). The fraction unbound in the extracellular and intracellular compartments was fixed to those currently measured in the plasma and liver. The initial concentration in the extracellular compartment was arbitrarily fixed at 1 μM and that of the intracellular compartment was fixed at 0 μM. To evaluate the role of uptake transporter expression, recent data comparing OATP expression in unplated monkey hepatocytes to that in liver tissue were used to scale Cl_{up} from that measured in hepatocytes to that in the liver (Wang et al., 2014). Given similar reported K_m values for rosuvastatin uptake by cynomolgus monkey OATP1B1 and OATP1B3 and a similar expression in monkey liver (Shen et al., 2013; Wang et al., 2014), contribution of these two transporters was considered equal. OATP2B1 activity was not considered as the same recent report determined its expression was negligible in monkeys compared with OATP1B1 and OATP1B3. Equation 10 was used to calculate liver active uptake clearance

$$Clup_{\text{liver}} = Clup_{\text{hepatocyte (in vivo)}} \frac{\text{OATP1B1/OATP1B3 expression in liver}}{\text{OATP1B1/OATP1B3 expression in hepatocytes}} \quad (10)$$

where $Clup_{\text{hepatocyte(in vivo)}}$ represents in vivo unbound Cl_{up} scaled directly from in vitro hepatocyte uptake, and $Clup_{\text{liver}}$ represents the scaled in vivo unbound Cl_{up} after accounting for hepatocyte-to-liver differences in transporter expression. Simulations were then carried out by replacing the value for Cl_{up} with Cl_{liver} in the model. A scaling factor for PS_{diff} was also considered. Using rat hepatocytes, PS_{diff} for seven compounds was reported higher in suspension than in short-term culture (Yabe et al., 2011; Menochet et al., 2012a), with a mean difference of 6-fold. Simulations were then carried out assuming a 6-fold lower value on PS_{diff}. Finally, many publications have called into question the restriction of drug-transporter interaction by extracellular protein binding (Burczynski et al., 2001; Blanchard et al., 2006; Poulin et al., 2012). Therefore, simulations were also carried out assuming active uptake transport was not limited by extracellular protein binding by removing this parameter from Cl_{up} in model equations.

Results

In Vivo Rosuvastatin Liver Kp, Binding, and $Kp_{u,u}$ in Monkeys. Individual plasma and liver rosuvastatin concentrations following oral administration in monkeys are displayed in Fig. 2. Liver concentrations greatly exceeded plasma concentrations, with individual Kp values for each set of livers and corresponding plasma samples ranging from 69 to 145. Partitioning was similar at each time point, indicating hepatic transport had reached equilibrium at the time points assessed. Using overall area under the concentration time curve values, the value for total Kp was 118. The calculated rosuvastatin fraction unbound in the plasma and liver were both 0.12, resulting in an in vivo $Kp_{u,u}$ value of 118. Calculated fraction unbound in hepatocytes at 15 × 10⁶ cells/ml was similar to that in the liver (0.13). Undiluted fraction unbound values at lower hepatocyte concentrations were considered invalid, as undiluted fraction unbound becomes imprecise when the measured fraction unbound approaches 80% (Pfeifer et al., 2013), and these values were 77 and 86% at 1 and 5 × 10⁶ cells/ml, respectively.

Prediction of In Vivo Liver Partitioning from In Vitro Hepatocyte Uptake. As shown in Fig. 3A, uptake at 4°C and that
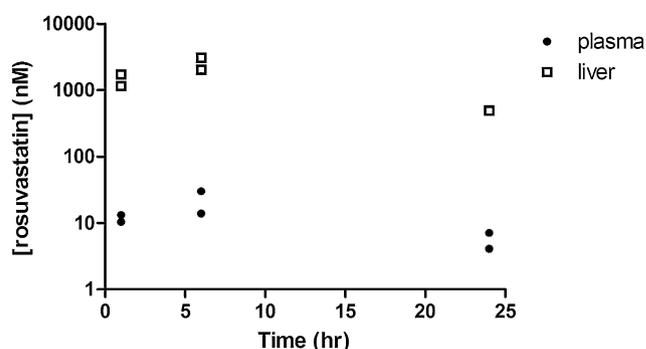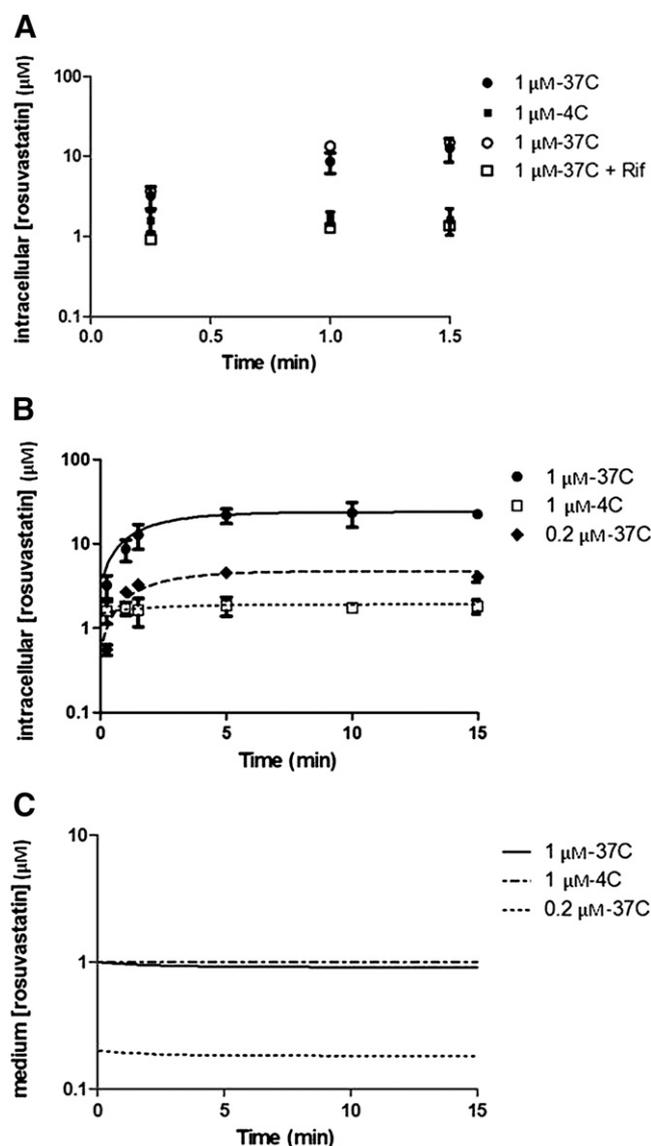

Fig. 2. Rosuvastatin liver and plasma concentrations following oral administration to cynomolgus monkeys. Monkeys ($n = 3$) were administered rosuvastatin 3 mg/kg by oral gavage on two study days. On each study day, plasma was collected at 1, 6, and 24 hours from all monkeys and one liver sample from one monkey was taken per study day. Data presented are corresponding plasma and liver samples taken over two study days.

with rifamycin were overlapping, indicating passive diffusion of rosuvastatin is similar at 4 and 37°C. In vitro model fitting is shown in Fig. 3B, indicating a good fit of data at 37 and 4°C by the two-compartment model. Simulated medium concentrations are shown in Fig. 3C, verifying little change over time as presumed, assuming mass balance is maintained. The fitted in vitro values for fu_{cell}, Cl_{up}, and PS_{diff} were 0.50 (7%), 54.5 (8%) μl/10⁶ cells/min, and 4.48 (13%) μl/10⁶ cells/min, respectively. The coefficient of variation for each parameter in parentheses indicated the model was able to estimate Cl_{up}, PS_{diff}, and fu_{cell} simultaneously with good precision. Using this fitted fu_{cell} value, the calculated value for in vitro $Kp_{u,u}$ was 12, underestimating in vivo $Kp_{u,u}$ by ~10-fold.

The effect of varying fu_{cell} values on fitted clearance parameters is displayed in Fig. 4. When fu_{cell} was fixed, Cl_{up} and PS_{diff} could be reliably estimated using only the 37°C data (coefficient of variation < 20% for both parameters). As shown, imprecision of fu_{cell} when the value is high (≥ 0.5) has little effect on rosuvastatin Cl_{up} or PS_{diff}; however, imprecision in this parameter at low values appears to greatly affect both clearance parameter estimations. Fixing the rosuvastatin fu_{cell} to a lower value than the true value in the in vitro system would underestimate Cl_{up}, overestimate PS_{diff}, and therefore underestimate $Kp_{u,u}$. Fixing fu_{cell} to the highest value of 1 resulted in a $Kp_{u,u}$ of 25, which is still underpredicting in vivo $Kp_{u,u}$ by ~5-fold.
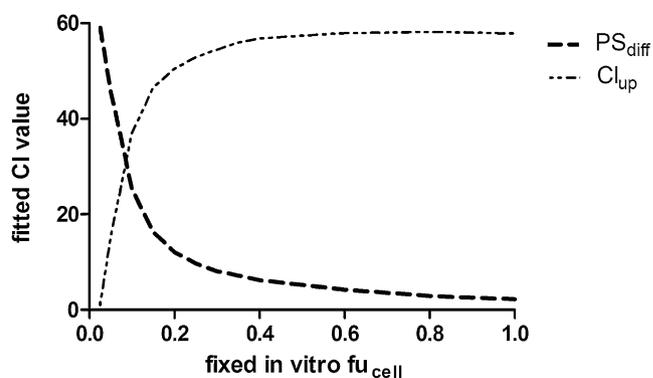
Model Simulations to Hypotheses Underlying the Underprediction of In Vivo $Kp_{u,u}$. As shown in Table 1, when the clearance values, volumes, and binding parameters were fixed to those resembling plasma and liver, in contrast to in vitro studies, a decrease in extracellular (plasma) rosuvastatin concentrations could be observed at steady state compared with that initially, as would be with systemic rosuvastatin administration in vivo. Given maintenance of the ratio of active and passive clearances from those determined in vitro, the in vivo $Kp_{u,u}$ was still similarly underestimated by ~10-fold. Correcting Cl_{up} for the reported hepatocyte-to-liver OATP expression made no significant improvement on this underprediction. Corrections on PS_{diff} and assuming active transport is not limited by protein binding improved $Kp_{u,u}$ estimation similarly to that observed in vivo. This suggests differences between membrane permeability in vitro and in vivo and that plasma protein binding may not limit active transport. Interestingly, with the volumes scaled to those of plasma and liver, the corrections that affected $Kp_{u,u}$ significantly affected the extracellular (plasma) steady-state concentrations, with little effect on those in the intracellular (liver) compartment.

Fig. 4. Effect of fixed fu_{cell} values on fitted clearance parameters. The parameter fu_{cell} was fixed to values ranging from 0.05 to 1, and at each fixed fu_{cell} value, the Cl_{up} and PS_{diff} parameters were estimated using the two-compartment model described in Fig. 1 using uptake at 37°C only.

Fig. 3. Rosuvastatin uptake in monkey hepatocytes. (A) Comparison of rosuvastatin uptake at 37 and 4°C with that at 37°C with and without 100 μM rifamycin SV (mean ± S.D.). Closed and open symbols represent two different experiments. (B) Observed (symbols, mean) and fitted (lines) rosuvastatin uptake at 37 and 4°C. All data were fit simultaneously. (C) Simulated medium concentrations from resulting fitted model parameters.

Discussion

Assessing drug concentrations and partitioning in target tissues is crucial to understanding pharmacokinetic/pharmacodynamic relationships for drug efficacy, drug-drug interactions, and off-target toxicity. Although the hepatocyte partitioning of multiple compounds has been evaluated in vitro and in situ in rodents, we present an initial evaluation of the translation of these in vitro methods to in vivo data in cynomolgus monkeys. In utilizing in vitro to in vivo extrapolation for the prediction of plasma concentrations, whether by metabolism or transport, underestimation by in vitro methods is a well known issue in drug development (Galetin, 2014). Specifically, using physiologically based pharmacokinetic modeling, prediction of in vivo plasma uptake clearance for OATP substrates in humans from in vitro hepatocyte uptake requires empirical scaling factors to account for underprediction in vitro (Poirier et al., 2009; Jones et al., 2012). Previous estimates evaluate prediction of human plasma data only, however, and conclusions about in vitro to in

vivo prediction of hepatic accumulation cannot be made, whereas the liver remains the site of action for many transporter substrates. In the present work, we present a method of liver sampling that allows for the collection of plasma and liver over time in monkeys and report an underprediction of unbound steady-state hepatic partitioning for rosuvastatin using cryopreserved hepatocytes in a species with a similar OATP homology and activity as that in humans (Shen et al., 2013).

Although calculation of total drug partitioning in vitro and in vivo is relatively straightforward, the accurate determination of the intracellular unbound fraction is essential for indirect determination of $Kp_{u,u}$ from Kp. In vivo tissue unbound fraction is traditionally determined by measurement using equilibrium dialysis in diluted homogenate or cell lysate of the tissue of interest (Mariappan et al., 2013), as performed in the current study. In silico methods have been also used for the prediction of in vivo tissue unbound fraction and tissue partitioning (Poulin and Theil, 2000). The use of the currently measured binding value of 0.12 for fu_{liver} is supported by the similar fraction unbound determined in hepatocyte lysate (at a density of 15×10^6 cells/ml). Multiple approaches have been described for the determination of in vitro fu_{cell} using hepatocytes (Yabe et al., 2011; Menochet et al., 2012a; Shitara et al., 2013). The in vitro value estimated currently with the two-compartment model of 0.50 agrees with those previously determined in rat hepatocytes of 0.48 and 0.51 (Yabe et al., 2011; Menochet et al., 2012a). An interesting observation is that the in vitro fu_{cell} estimate in this work is higher than the measured fu_{liver}. Due to saturation of nonspecific binding sites in vitro, the in vitro fu_{cell} may overestimate the true value in tissue (Zamek-Gliszczynski et al., 2013). The importance of understanding the in vitro fu_{cell} parameter is emphasized in Fig. 4, in which applying too low of a value, such as that directly measured in tissue, could greatly affect both active and passive values and further underestimate the $Kp_{u,u}$. In the current analysis, even assuming the largest in vitro fu_{cell} value of 1 for rosuvastatin, the in vitro data still underpredict the in vivo $Kp_{u,u}$ by 5-fold, indicating that even in the uncertainty of in vitro fu_{cell}, there still exists an in vitro to in vivo discrepancy in the prediction of unbound hepatocyte partitioning.

The utility of modeling of the in vitro uptake has been recently emphasized as it allows simultaneous determination of multiple clearance parameters and intracellular unbound fraction (Zamek-Gliszczynski et al., 2013). A further benefit of employing mathematical modeling is the ability to perturb parameters and test hypotheses. As mentioned, previous efforts investigating the extrapolation of in vitro transport parameters to those in vivo using physiologically based modeling have concluded a need for scaling factors on in vitro Cl_{up} to accurately predict in vivo plasma data,

TABLE 1

Values used for model simulations and resulting predicted steady-state rosuvastatin concentrations and partitioning

Clearance parameters were scaled from those determined in the in vitro model to represent those in the liver of a 5-kg monkey. Volumes for the extracellular and intracellular compartments were fixed to those of the plasma and liver, respectively, of a 5-kg monkey. Extracellular and intracellular fu were fixed to those measured in monkey plasma and liver, respectively. The initial condition for C_{EC} and C_{IC} was arbitrarily fixed to 1 and 0 μM, respectively.

	PS_{diff}	Cl_{up}	fu_{EC}	fu_{IC}	C_{EC}	C_{IC}	Kp	$Kp_{u,u}$
	ml/min	*ml/min*			*μM*	*μM*		
Scaled in vitro model parameters	82	1010	0.12	0.12	0.11	1.4	12	12
Corrected for transporter expression	82	1147	0.12	0.12	0.10	1.5	15	15
Corrected for cell surface area	14	1010	0.12	0.12	0.011	1.6	74	74
Active uptake not limited by binding	82	1010	0.12[a]	0.12	0.015	1.6	106	106

EC = extracellular; IC = intracellular.
[a]Removed from Cl_{up}.

including analyses specifically on rosuvastatin (Jones et al., 2012; Jamei et al., 2014). Several hypotheses for this have hence been generated, including low transporter expression/activity in vitro and the possibility of OATP expression at other sites in vivo (e.g., muscle) causing the high apparent in vivo plasma clearance. Although our data cannot rule out the involvement of other tissues, we can confirm with the current data that hepatic uptake is underestimated in vitro and that OATP expression elsewhere cannot be the sole cause for the necessity of an empirical scalar for rosuvastatin. To reconcile underprediction in vitro, we first attempted to integrate in vitro and in vivo OATP expression in monkey tissues, which unsurprisingly did not resolve the in vitro to in vivo discrepancy, given that reported OATP expression in isolated hepatocytes is almost 90% of that determined in the liver (Wang et al., 2014). The accurate estimation of passive diffusion is often neglected for clearance prediction of drugs in which active transport plays a large role; however, the value of PS_{diff} can be critical for the estimation of tissue partitioning. Given that the architecture of plated hepatocytes likely more closely represents that in vivo, we attempted scaling PS_{diff} using a previously reported difference for seven drugs in suspension versus short-term plated hepatocytes. With the application of this scaling factor, the in vitro to in vivo disconnect on $Kp_{u,u}$ was almost eliminated. Another assumption in all clearance prediction is that only the unbound drug is available for permeation or metabolism. This has been challenged, however, as it has been demonstrated that plasma protein interactions at the cell surface may actually increase drug permeability (Poulin et al., 2012). Furthermore, for many transporter substrates, hepatic extraction is high despite their low unbound fraction. For example, for most statins, hepatic extraction is ≥70%, whereas the unbound fraction in the plasma is ≤10%, suggesting protein binding is not limiting for OATP-mediated hepatic extraction of these drugs (Igel et al., 2002). Removing this assumption on the protein binding effects was completely able to reconcile the underprediction of in vivo $Kp_{u,u}$ from in vitro data; however, it is likely that in vivo plasma protein binding cannot be completely discounted and differences in affinity between transporter and plasma proteins may need to be considered. Given that $Kp_{u,u}$ could hypothetically be reconciled through scaling of any of multiple parameters, it must be noted that the observed underprediction for rosuvastatin may not be quantitatively similar for other OATP substrates possessing different physicochemical properties and/or also undergoing metabolism. Prediction of plasma clearance for OATP substrates from in vitro data has demonstrated the need for drug-dependent scalars (Jones et al., 2012). Furthermore, use of different scalars or scaling of different parameters may be needed for substrates of other hepatic transporters, such as organic cation transporter 1, as hepatocyte isolation may have differing effects on the expression of various transporters (Soars et al., 2009; Lundquist et al., 2014). Overall, the simulation results warrant further investigations on the exact mechanisms contributing to the underestimation of unbound partitioning in vitro, including evaluation of a wider range of transporter substrates.

In summary, we present a novel methodology for the determination of in vivo drug liver partitioning in cynomolgus monkeys via ultrasound-guided biopsy. Using this technique, unbound liver partitioning of rosuvastatin in monkeys was extensive, further confirming the role of active hepatic uptake transporters in rosuvastatin hepatic accumulation in this species. Although in vitro hepatocyte uptake predicted the presence of active uptake and a $Kp_{u,u}$ greater than unity, current in vitro methods were not able to quantitatively predict unbound partitioning in vivo, with a 10-fold underprediction. Multiple explanations for this in vitro underprediction exist, which need to be further explored. In vitro to in vivo extrapolation of other compounds needs to be evaluated using similar methods to determine if underprediction of $Kp_{u,u}$ is similar in monkeys for substrates of other hepatic transporters or OATP substrates undergoing multiple processes, including enzyme metabolism.

Authorship Contributions

Participated in research design: Lai, Cai, Shu, Morse, L. Zhang, Shen, Dierks, MacGuire, Marathe, Su.

Conducted experiments: MacGuire, Fox, Luk, Cai, Y. Zhang, L. Zhang, Morse, Su, Gu.

Contributed new reagents or analytic tools: MacGuire, Dierks, Lai, Cai.

Performed data analysis: Morse, Cai, L. Zhang, Y. Zhang, Shen, Shu, Lai.

Wrote or contributed to the writing of the manuscript: Morse, Lai, MacGuire, Marathe, Humpheys, Cai.

References

Bauer M, Zeitlinger M, Karch R, Matzneller P, Stanek J, Jäger W, Böhmdorfer M, Wadsak W, Mitterhauser M, and Bankstahl JP, et al. (2012) Pgp-mediated interaction between (R)-[11C] verapamil and tariquidar at the human blood-brain barrier: a comparison with rat data. *Clin Pharmacol Ther* **91**:227–233.

Berry MN and Friend DS (1969) High-yield preparation of isolated rat liver parenchymal cells: a biochemical and fine structural study. *J Cell Biol* **43**:506–520.

Bischoff KB, Dedrick RL, Zaharko DS, and Longstreth JA (1971) Methotrexate pharmacokinetics. *J Pharm Sci* **60**:1128–1133.

Blanchard N, Hewitt NJ, Silber P, Jones H, Coassolo P, and Lavé T (2006) Prediction of hepatic clearance using cryopreserved human hepatocytes: a comparison of serum and serum-free incubations. *J Pharm Pharmacol* **58**:633–641.

Burczynski FJ, Wang GQ, Elmadhoun B, She YM, Roberts MS, and Standing KG (2001) Hepatocyte [3H]-palmitate uptake: effect of albumin surface charge modification. *Can J Physiol Pharmacol* **79**:868–875.

Chu X, Bleasby K, and Evers R (2013a) Species differences in drug transporters and implications for translating preclinical findings to humans. *Expert Opin Drug Metab Toxicol* **9**:237–252.

Chu X, Korzekwa K, Elsby R, Fenner K, Galetin A, Lai Y, Matsson P, Moss A, Nagar S, and Rosania GR, et al.; International Transporter Consortium (2013b) Intracellular drug concentrations and transporters: measurement, modeling, and implications for the liver. *Clin Pharmacol Ther* **94**:126–141.

Galetin A (2014) Rationalizing underprediction of drug clearance from enzyme and transporter kinetic data: from in vitro tools to mechanistic modeling. *Methods Mol Biol* **1113**:255–288.

Hagenbuch B and Meier PJ (2004) Organic anion transporting polypeptides of the OATP/ SLC21 family: phylogenetic classification as OATP/ SLCO superfamily, new nomenclature and molecular/functional properties. *Pflugers Arch* **447**:653–665.

Houston JB (1994) Utility of in vitro drug metabolism data in predicting in vivo metabolic clearance. *Biochem Pharmacol* **47**:1469–1479.

Igel M, Sudhop T, and von Bergmann K (2002) Pharmacology of 3-hydroxy-3-methylglutaryl-coenzyme A reductase inhibitors (statins), including rosuvastatin and pitavastatin. *J Clin Pharmacol* **42**:835–845.

Jamei M, Bajot F, Neuhoff S, Barter Z, Yang J, Rostami-Hodjegan A, and Rowland-Yeo K (2014) A mechanistic framework for in vitro-in vivo extrapolation of liver membrane transporters: prediction of drug-drug interaction between rosuvastatin and cyclosporine. *Clin Pharmacokinet* **53**:73–87.

Jones HM, Barton HA, Lai Y, Bi YA, Kimoto E, Kempshall S, Tate SC, El-Kattan A, Houston JB, and Galetin A, et al. (2012) Mechanistic pharmacokinetic modeling for the prediction of transporter-mediated disposition in humans from sandwich culture human hepatocyte data. *Drug Metab Dispos* **40**:1007–1017.

Kalvass JC and Maurer TS (2002) Influence of nonspecific brain and plasma binding on CNS exposure: implications for rational drug discovery. *Biopharm Drug Dispos* **23**:327–338.

Keemink J, Augustijns P, and Annaert P (2015) Unbound ritonavir concentrations in rat and human hepatocytes. *J Pharm Sci* **104**:2378–2387.

Lundquist P, Lööf J, Sohlenius-Sternbeck AK, Floby E, Johansson J, Bylund J, Hoogstraate J, Afzelius L, and Andersson TB (2014) The impact of solute carrier (SLC) drug uptake transporter loss in human and rat cryopreserved hepatocytes on clearance predictions. *Drug Metab Dispos* **42**:469–480.

Mariappan TT, Mandlekar S, and Marathe P (2013) Insight into tissue unbound concentration: utility in drug discovery and development. *Curr Drug Metab* **14**:324–340.

Ménochet K, Kenworthy KE, Houston JB, and Galetin A (2012a) Simultaneous assessment of uptake and metabolism in rat hepatocytes: a comprehensive mechanistic model. *J Pharmacol Exp Ther* **341**:2–15.

Ménochet K, Kenworthy KE, Houston JB, and Galetin A (2012b) Use of mechanistic modeling to assess interindividual variability and interspecies differences in active uptake in human and rat hepatocytes. *Drug Metab Dispos* **40**:1744–1756.

Nordell P, Winiwarter S, and Hilgendorf C (2013) Resolving the distribution-metabolism interplay of eight OATP substrates in the standard clearance assay with suspended human cryopreserved hepatocytes. *Mol Pharm* **10**:4443–4451.

Paine SW, Parker AJ, Gardiner P, Webborn PJ, and Riley RJ (2008) Prediction of the pharmacokinetics of atorvastatin, cerivastatin, and indomethacin using kinetic models applied to isolated rat hepatocytes. *Drug Metab Dispos* **36**:1365–1374.

Pfeifer ND, Harris KB, Yan GZ, and Brouwer KL (2013) Determination of intracellular unbound concentrations and subcellular localization of drugs in rat sandwich-cultured hepatocytes compared with liver tissue. *Drug Metab Dispos* **41**:1949–1956.

Poirier A, Cascais AC, Funk C, and Lavé T (2009) Prediction of pharmacokinetic profile of valsartan in human based on in vitro uptake transport data. *J Pharmacokinet Pharmacodyn* **36**:585–611.

Poirier A, Lavé T, Portmann R, Brun ME, Senner F, Kansy M, Grimm HP, and Funk C (2008) Design, data analysis, and simulation of in vitro drug transport kinetic experiments using a mechanistic in vitro model. *Drug Metab Dispos* **36**:2434–2444.

Poulin P, Kenny JR, Hop CE, and Haddad S (2012) In vitro-in vivo extrapolation of clearance: modeling hepatic metabolic clearance of highly bound drugs and comparative assessment with existing calculation methods. *J Pharm Sci* **101**:838–851.

Poulin P and Theil FP (2000) A priori prediction of tissue:plasma partition coefficients of drugs to facilitate the use of physiologically-based pharmacokinetic models in drug discovery. *J Pharm Sci* **89**:16–35.

Reinoso RF, Telfer BA, Brennan BS, and Rowland M (2001) Uptake of teicoplanin by isolated rat hepatocytes: comparison with in vivo hepatic distribution. *Drug Metab Dispos* **29**:453–459.

Shen H, Su H, Liu T, Yao M, Mintier G, Li L, Fancher RM, Iyer R, Marathe P, and Lai Y, et al. (2015) Evaluation of rosuvastatin as an organic anion transporting polypeptide (OATP) probe substrate: in vitro transport and in vivo disposition in cynomolgus monkeys. *J Pharmacol Exp Ther* **353**:380–391.

Shen H, Yang Z, Mintier G, Han YH, Chen C, Balimane P, Jemal M, Zhao W, Zhang R, and Kallipatti S, et al. (2013) Cynomolgus monkey as a potential model to assess drug interactions involving hepatic organic anion transporting polypeptides: in vitro, in vivo, and in vitro-to-in vivo extrapolation. *J Pharmacol Exp Ther* **344**:673–685.

Shitara Y, Maeda K, Ikejiri K, Yoshida K, Horie T, and Sugiyama Y (2013) Clinical significance of organic anion transporting polypeptides (OATPs) in drug disposition: their roles in hepatic clearance and intestinal absorption. *Biopharm Drug Dispos* **34**:45–78.

Soars MG, Webborn PJ, and Riley RJ (2009) Impact of hepatic uptake transporters on pharmacokinetics and drug-drug interactions: use of assays and models for decision making in the pharmaceutical industry. *Mol Pharm* **6**:1662–1677.

van Velden FH, Mansor SM, van Assema DM, van Berckel BN, Froklage FE, Wang S, Schuit RC, Asselin MC, Lammertsma AA, and Boellaard R, et al. (2015) Comparison of HRRT and HR+ scanners for quantitative (R)-[11C]verapamil, [11C]raclopride and [11C]flumazenil brain studies. *Mol Imaging Biol* **17**:129–139.

Wang L, Prasad B, Salphati L, Chu X, Gupta A, Hop CE, Evers R, and Unadkat JD (2014) Interspecies variability in expression of hepatobiliary transporters across human, dog, monkey and rat as determined by quantitative proteomics. *Drug Metab Dispos* **43**:367–374.

Yabe Y, Galetin A, and Houston JB (2011) Kinetic characterization of rat hepatic uptake of 16 actively transported drugs. *Drug Metab Dispos* **39**:1808–1814.

Zamek-Gliszczynski MJ, Lee CA, Poirier A, Bentz J, Chu X, Ellens H, Ishikawa T, Jamei M, Kalvass JC, and Nagar S, et al.; International Transporter Consortium (2013) ITC recommendations for transporter kinetic parameter estimation and translational modeling of transport-mediated PK and DDIs in humans. *Clin Pharmacol Ther* **94**:64–79.

Address correspondence to: Yurong Lai, Route 206 and Provinceline Rd, Princeton, NJ 08540. E-mail: yurong.lai@bms.com